CONTROL OF LONGITUDINAL TENSION IN MULTI-SPAN WEB TRANSPORT SYSTEMS DURING START UP

Karl N. Reid and Ku-Chin Lin

School of Mechanical and Aerospace Engineering
Oklahoma State University
Stillwater, Oklahoma

ABSTRACT

The control of longitudinal tension in a multi-span web transport system during start up is studied using first-principles modeling and digital simulation. Since start-up problems normally involve large variations of system roller velocities, nonlinear models (rather than linearized models) are used for the analysis.

Examples of systems using load cells and dancer subsystems for tension measurement are presented to demonstrate the effects on web tension of changes in the start-up conditions.

NOMENCLATURE

A	Cross-sectional area of web
b	Width of web
e	Error signal
E	Modulus of elasticity
h	Thickness of web
J	Moment of inertia of a roll or roller
K	Motor (or, brake) torque constant
K_p	Proportional gain
K_i	Integral gain
K_d	Derivative gain
L	Length of web span
L_a	Length of the lever arm in a pivoting dancer subsystem
M	Mass of roller
R	Radius of roll or roller

s	Distance measured along the web
S	Laplace operator
t	Web tension
T	Change in web tension from a steady-state value
u	Motor (Brake) input current
v	Roller velocity
V	Change in web velocity from a steady-state value
X	Change in linear displacement of dancer roller
δ	Displacement of web in the machine direction
ε	Web strain
θ	Angle of wrap of web over a roller
τ	Time
τ_r	Rise time
τ_s	Start-up time
ω	Roller angular velocity
Ω	Natural frequency
ζ	Damping ratio

Subscripts:

i	Initial steady state
j	dummy index
m	1,2,3, . . .
n	1,2,3, . . .
o	Process condition (or, initial condition)

Superscripts:

n	1,2,3, . . .
*	Reference (or, measured) signal

INTRODUCTION

Web breakage and/or slackness can occur during the start up of a web transport system if the web tension[1] in each span is improperly controlled. Modeling and simulation tools can be used to study the dynamic behavior of the system during start up prior to system construction. In this study, the system can be designed with precise control of web tension in each span during the start-up transient.

Two examples are presented in this paper to illustrate the effects on web tension of changes in the start-up conditions. Two types of web tension measurement approaches are considered: a load cell subsystem and a dancer subsystem. Simple fixed-gain PID controllers are utilized. Several cases are studied in each example which illustrate that variable-gain controllers are needed to produce good dynamic behavior over a broad range of start-up conditions.

DYNAMICS OF A WEB SPAN

[1] Throughout this paper, the term "tension" refers to the longitudinal tension of web

Figure 1 shows a schematic diagram of a web span. If it is assumed that no slippage occurs between the rollers and web, the law of conservation of mass can be written as:

$$\frac{d}{d\tau}\int_0^{L_n} \rho_n A_n \, ds = \rho_{n-1} A_{n-1} v_n - \rho_n A_n v_{n+1} . \quad (1)$$

If the web is assumed perfectly elastic, Hooke's law can be written as:

$$t_n = A_n E_n \varepsilon_n , \quad (2)$$

where $\varepsilon_n \equiv \delta_n / L_n$ and δ_n denotes the stretched or compressed displacement of the web in the machine direction.

Through considering an infinitesimal element in the web span of length ds, Equations (1) and (2) can be combined to give the following nonlinear differential equation (3):

$$L_n \dot{t}_n = v_{n+1}(E_n A_n - t_n) - v_n(E_n A_n - t_{n-1}) . \quad (3)$$

Equation (3) can be linearized if it is assumed that all variables undergo small perturbations from initial steady-state values. The result is:

$$L_n \dot{T}_n = - v_{n+1,o} T_n + v_{n,o} T_{n-1} + E_n A_n (V_{n+1} - V_n) . \quad (4)$$

Equation (4) shows that the tension in a web span is created by the velocity difference between the ends of the web span. The tension in a span also depends on the incoming web tension, i.e., tension is transferred from an upstream span to a downstream span in a web transport system.

Equation (4) is useful in the study of system steady-state and dynamic behavior when changes in variables are sufficiently small. However, Equation (3) must be considered in this study because changes in the roller velocities are normally large during the process of start up.

DYNAMICS OF A ROLLER

Figure 2(a) shows a schematic diagram of a passive roller (e.g., an idle roller or a dancer roller) and its adjacent web spans. If it is assumed that the bearing friction in the roller is negligible, a torque balance on the roller gives:

$$J_n \dot{\omega}_n = R_n (t_n - t_{n-1}) . \quad (5)$$

For a non-passive roller (e.g., unwinding roll, driven roller, or winding roll) as shown in Fig. 2(b), the torque balance equation is

$$J_n \dot{\omega}_n = R_n (t_n - t_{n-1}) + K_n u_n , \quad (6)$$

where $K_n u_n$ denotes the torque generated by the motor (brake) which is attached to the non-passive roller.

CONTROL OF WEB TENSION USING LOAD CELLS FOR TENSION MEASUREMENT

Consider the system shown in Fig. 3. Local feedback control systems are used to accurately control tension in each of two spans and the speed of the driven roller (master speed control).

System Modeling

Figure 3 shows a schematic representation of a simplified web transport system which includes, from the left to the right, an unwinding roll, a load cell, a driven roller, a load cell, and a winding roll.

The dynamics of each roller (roll) and span of web in Fig. 3 can be modeled using Equations (3), (5), and (6). The system equations are arranged below in the order of the unwinding roll, the first span, the first load cell roller, and so on:

$$J_1(\tau)\,\dot{v}_1 = -R_1(\tau)\,K_1\,u_1 + R_1^2(\tau)\,t_1 \tag{7}$$

$$E_1\,\dot{t}_1 = v_2(E_1\,A_1 - t_1) - v_1(E_1\,A_1 - K_1\,u_1/R_1(\tau)) \tag{8}$$

$$J_2\,\dot{v}_2 = R_2^2\,(t_2 - t_1) \tag{9}$$

$$L_2\,\dot{t}_2 = v_3(E_2\,A_2 - t_2) - v_2(E_2\,A_2 - t_1) \tag{10}$$

$$J_3\,\dot{v}_3 = R_3^2\,(t_3 - t_2) + R_3\,K_3\,u_3 \tag{11}$$

$$L_3\,\dot{t}_3 = v_4(E_3\,A_3 - t_3) - v_3(E_3\,A_3 - t_2) \tag{12}$$

$$J_4\,\dot{v}_4 = R_4^2\,(t_4 - t_3) \tag{13}$$

$$L_4\,\dot{t}_4 = v_5(E_4\,A_4 - t_4) - v_4(E_4\,A_4 - t_3) \tag{14}$$

$$J_5(\tau)\,\dot{v}_5 = -R_5^2(\tau)\,t_4 + R_5(\tau)\,K_5\,u_5 \tag{15}$$

where the radii of the unwinding and winding rolls are time-varying:

$$R_1(\tau) = \sqrt{R_{1i}^2 - \frac{v_1\,h\,\tau}{\pi}}\,, \tag{16}$$

$$R_5(\tau) = \sqrt{R_{5i}^2 + \frac{v_5\,h\,\tau}{\pi}}\,, \tag{17}$$

and R_{1i} denotes the initial radius of the unwinding roll; R_{5i} the initial radius of the winding roll.

System Controllers

In Fig. 3, the process speed is controlled by the driven roller (i.e., a master-speed roller) with a PI controller. PID controllers are used to control the web tensions in the unwinding and winding sections. The three controllers are described as follows:

$$u_1 = (K_{p1} + K_{i1} \int_0^\tau d\tau + K_{d1} \frac{d}{d\tau}) e_1 \tag{18}$$

$$u_3 = (K_{p3} + K_{i3} \int_0^\tau d\tau) e_3 \tag{19}$$

$$u_5 = (K_{p5} + K_{i5} \int_0^\tau d\tau + K_{d5} \frac{d}{d\tau}) e_5 \tag{20}$$

where

$$e_1 = t_2^* - (t_1 + t_2)/2 \ , \tag{21}$$

$$e_3 = v_3^* - v_3 \ , \tag{22}$$

$$e_5 = t_4^* - (t_3 + t_4)/2 \ . \tag{23}$$

The different P, I, and D gains can be determined by tuning, or one of several well-known linear system methods.

In the design of the PID gains for the examples in this paper, the dynamics of the load cell rollers shown in Fig. 3 are neglected. The gains are designed based on the linearization of the system equations around an operating condition and the pole assignment technique (3). With this approach, the design of the PID gains is equivalent to the design of the roots of the following characteristic equation of a reference third-order system:

$$(S + K_r \zeta \Omega) (S^2 + 2 \zeta \Omega S + \Omega^2) = 0 \tag{24}$$

where if the constant K_r is large (i.e., the real pole, $-K_r \zeta \Omega$, is not dominant), the third-order system is similar to a second-order system with a damping ratio ζ and a natural frequency Ω.

In this paper, the damping ratio and the rise time τ_r (rather than the natural frequency) of a reference second-order system are considered as design parameters. The following equation can be used for the calculation of the natural frequency for a given damping ratio and rise time (2):

$$\Omega = \frac{1 + 1.1 \zeta + 1.4 \zeta^2}{\tau_r} \tag{25}$$

It is the primary purpose of this paper to investigate the robustness of PID controllers with fixed gains when there are changes of the radii and moments of

inertia of the unwinding and winding rolls.

Example 1 - System with Load Cells for Tension Measurement

Consider the start up of the system shown in Fig. 4 as a result of the ramp input shown in Fig. 5. The system starts at a web velocity of zero and reaches a web velocity of 5 m/sec (1000 fpm) after τ_s seconds. The system equations were simulated for three cases. The initial web tension is 1 pli (i.e., 1 lbf per linear inch of web width) for all cases.

Case 1:

R_{1i} = 0.607 m (2.0 ft), J_{1i} = 21.192 N-m-sec^2 (15.1 ft-lbf-sec^2)
R_{5i} = 0.152 m (0.5 ft), J_{5i} = 0.083 N-m-sec^2 (0.059 ft-lbf-sec^2)
other parameters and initial conditions are given in the Appendix

For illustrative purposes, it is desired to design controlled responses of web tension with a damping ratio of $\zeta = 0.75$, a rise time of $\tau_r = 0.15$ second, and K_r = 20. The PID gains were calculated based on these design parameters using the linearization and pole assignment techniques mentioned in the previous section.

Figures 5(a), 5(b), and 5(c) show the time responses of the control inputs, roller velocities, and web tensions respectively. From Fig. 5(b), the roller velocities are essentially the same throughout the start-up period. Since the dynamics of the web spans are far faster than those of the rollers and the motors, the time required for each roller to adapt itself to the input v_3^* is much shorter than the start-up time (i.e., τ_s).

Figure 5(c) indicates that at the initiation of the ramp input v_3^* (or, the deactivation of the ramp input), the web tension t_1 is affected by the acceleration (deceleration) of the first load cell roller which is due to the increase (decrease) of t_2. The web tension is also affected by the decrease (increase) of the brake torque because of the PID control. Both affects have the reverse contribution to the value of t_1.

There is a time delay for the control action. This delay can be reduced by increasing the PID gains. However, this control delay is the primary reason why the response of t_1 and similarly why the response of t_4 shown in Fig. 5(c) are undershoots at the beginning and the end of the system start up.

Figure 5(c) also shows that the responses of t_1 and t_2 to the ramp change of v_3^* reach "steady states" where the average of t_1 and t_2 is equal to the reference tension t_2^*, and the tension difference $t_2 - t_1$ is equal to $J_2\dot{v}_2 / R_2^2$ (see Equation (5)).

Obviously, the responses of web tension shown in Fig. 5(c) are more oscillatory than what were designed. Further improvement of the damping of the responses can be achieved by tuning the PID gains as considered in the following case study:

Case 2: same as Case 1 except that the integral gains in the PID controllers which were designed for Case 1 are increased

As the integral gains in the PID controllers which were designed for Case 1 increase, the overshoots and undershoots of the tension responses shown in Fig. 5(c) are reduced. Figure 6 shows the time responses of system inputs and outputs

when the integral gains are four times those for Case 1.

The velocity responses shown in Fig. 6(b) are not much different from those for Case 1. However, the tension responses become more damped because of the increase of the integral gains.

The PID controllers for Case 2 are well tuned for the control of tension during the start up of the web transport system shown in Fig. 3 with a large unwinding roll and a small winding roll.

Case 3: same as Case 2 except

R_{1i} = 0.506 m (1.667 ft), J_{1i} = 10.235 N-m-sec^2 (7.293 ft-lbf-sec^2)

R_{5i} = 0.368 m (1.213 ft), J_{5i} = 2.845 N-m-sec^2 (2.027 ft-lbf-sec^2)

With the linear PID controllers which were tuned based on the system conditions of Case 2, the time responses of the control inputs, roller velocities, and web tensions change as the system start-up conditions change from Case 2 to Case 3. The responses are shown in Fig. 7(a), 7(b), and 7(c), respectively.

At the winding section, the PID controller, which was well tuned for a small roll, becomes detuned as the radius of the winding roll increases. The result is that the responses of t_3 and t_4 shown in Fig. 7(c) become sluggish.

The controller at the unwinding section, which was tuned for a large roll, becomes detuned as the radius of the unwinding roll decreases. In other words, the control gains are too large. As shown in Fig. 7(c), the responses of t_1 and t_2 demonstrate chattering during the start up. Moreover, start up of the system without retuning the PID gains will result in significant increases of the "amplitudes" of the tension responses if the radius of the unwinding roll is further reduced, and that may cause web breakage.

CONTROL OF WEB TENSION USING DANCER SUBSYSTEMS FOR TENSION MEASUREMENT

Consider the web transport system shown in Fig. 8. This system is identical to that shown in Fig. 3 except that the load cells are replaced by pivoting dancer subsystems for tension measurement as shown in Fig. 9. The counterweight in each pivoting dancer subsystem is set in balance with the weight of the dancer roller. The web tensions are in balance at the pivot with the force generated by the pneumatic cylinder.

System Modeling

The system equations for the system with load cells (i.e., Equations (7) through (15)) still apply for the system with dancer subsystems except that the dynamic equation for each web span (i.e., Equation (8), (10), (12), or (14)) needs to be modified to include the effects due to the linear displacement of the dancer rollers.

It is assumed that the changes in the displacements of the dancer rollers are very small (i.e., $X_2 << L_{a2}$ and $X_4 << L_{a4}$) where L_{a2} and L_{a4} denote the lengths of the lever arms in the first and second dancer subsystems, respectively. Also, the radii of the dancer rollers are assumed to be very small in comparison with the lengths of the lever arms (i.e., $R_2 << L_{a2}$, , and $R_4 << L_{a4}$).

Torque balances at the pivots yield the following linearized equations:

$$M_2 L_{a2} \ddot{X}_2 = - (T_1 + T_2) \sin(\frac{\theta_2}{2}) L_{a2} \tag{26}$$

$$M_4 L_{a4} \ddot{X}_4 = - (T_3 + T_4) \sin(\frac{\theta_4}{2}) L_{a4} \tag{27}$$

Modification of the web equations to include the effects due to the vertical displacement of the dancer rollers is discussed in the companion paper (4). The results are summarized below:

$$L_1 \dot{t}_1 = v_2(E_1 A_1 - t_1) - v_1(E_1 A_1 - K_1 u_1/R_1(\tau)) + E_1 A_1 \sin\frac{\theta_2}{2} (\frac{v_2}{L_1} X_2 + \dot{X}_2) \tag{28}$$

$$L_2 \dot{t}_2 = v_3(E_2 A_2 - t_2) - v_2(E_2 A_2 - t_1) + E_2 A_2 \sin\frac{\theta_2}{2} (\frac{v_3}{L_2} X_2 - \frac{v_2}{L_1} X_2 + \dot{X}_2) \tag{29}$$

$$L_3 \dot{t}_3 = v_4(E_3 A_3 - t_3) - v_3(E_3 A_3 - t_2) + E_3 A_3 \sin\frac{\theta_4}{2} (\frac{v_4}{L_3} X_4 + \dot{X}_4) \tag{30}$$

$$L_4 \dot{t}_4 = v_5(E_4 A_4 - t_4) - v_4(E_4 A_4 - t_3) + E_4 A_4 \sin\frac{\theta_4}{2} (\frac{v_5}{L_4} X_4 - \frac{v_4}{L_3} X_4 + \dot{X}_4) \tag{31}$$

In summary, Equations (7), (9), (11), (13), (15), and (26) through (31) are the system equations for the system with dancer subsystems shown in Fig. 8.

System Controllers

The PI controllers for the controlled systems in Fig. 3 and Fig. 8 are the same. But, for the system with dancer subsystems, the PID controllers are designed based on the feedback of changes in the displacement of the dancer rollers (rather than the web tensions) as shown in Fig. 8. The web tensions would be equal to the preset values which are in torque balance at the pivots with the forces generated by the pneumatic cylinders if the dancer rollers are controlled and maintained at their null positions.

The PID controllers in Fig. 8 are described as follows:

$$u_1 = (K_{p1} + K_{i1} \int_0^\tau d\tau + K_{d1} \frac{d}{d\tau}) e_1 , \tag{32}$$

$$u_5 = (K_{p5} + K_{i5} \int_0^\tau d\tau + K_{d5} \frac{d}{d\tau}) e_5 , \tag{33}$$

where the error signals are

$$e_1 = X_2^* - X_2 , \tag{34}$$

$$e_5 = X_4^* - X_4 , \tag{35}$$

and X_2^* and X_4^* denote the reference changes in vertical displacement of the dancer rollers. Equations (19), (22), and (32) through (35) are the system controllers for the system with dancer subsystems shown in Fig. 8.

In the design of the PID gains in Equations (32) and (33), the translational dynamics of the dancer rollers shown in Fig. 8 must be considered. First, the system equations are linearized around an operating condition. A fourth-order linear model describes the system dynamic behavior. The model is then reduced to a second-order model using the technique of model reduction (1). Finally, the PID controller is designed based on the reduced second-order model using the pole assignment technique mentioned previously.

Example 2

Consider the start up of the system shown in Fig. 8 as a result of the ramp input shown in Fig. 4. The system equations were simulated for three cases.

Case 1: same initial conditions as Example 1 - Case 1
$M_2 = 14.7$ kgm (3.2 lbm), $\theta_2 = 180^\circ$, $X_2^* = 0$
$M_4 = 14.7$ kgm (3.2 lbm), $\theta_4 = 180^\circ$, $X_4^* = 0$

For illustrative purposes, it is desired to design controlled responses of web tension with a damping ratio of $\zeta = 0.75$, a rise time of $\tau_r = 0.6$ second, and $K_r = 1.0$. The PID gains were calculated based on these design parameters and the use of the reduced linear model and pole assignment techniques mentioned in the previous section.

The time responses of the control inputs, roller velocities, and web tension for this case study are shown in Fig. 10(a), 10(b), and 10(c), respectively. The responses of tension at the upstream side of a dancer roller are less damped as shown in Fig. 10 (c), i.e., the response of t_1 is less damped than that of t_2 and the response of t_4 is less damped than that of t_3. This indicates that a dancer roller can reduce the effects due to the change of web tension occurring at one side transferred to the other side of the dancer roller.

The oscillatory responses of t_1 and t_4 can be improved by increasing the derivative gains in the PID controllers as illustrated in the following case study.

Case 2: same as Case 1 except that the derivative gains in the PID controllers which were designed for Case 1 are increased

As the derivative gains in the PID controllers which were designed for Case 1 increase, the responses of t_1 and t_4 shown in Fig. 10(c) gradually become well damped. Figure 11 shows the time responses of system inputs and outputs when the derivative gains are four times larger than those for Case 1. As shown in Fig. 11(c), the responses of t_1 and t_4 are as well damped as the other tension responses.

The PID controllers are well tuned for Case 2 . The robustness of such controllers with fixed gains against the change of the radii and moment of inertia of the unwinding and winding rolls are investigated through the following case study.

Case 3: same as Case 2 except
R_{1i} = 0.332 m (1.095 ft), J_{1i} = 1.903 N-m-sec^2 (1.356 ft-lbf-sec^2)
R_{5i} = 0.530 m (1.747 ft), J_{5i} = 12.251 N-m-sec^2 (8.729 ft-lbf-sec^2)

With the linear PID controllers which were tuned based on the system conditions of Case 2, the time responses of the control inputs, roller velocities, and web tensions change as the system start-up conditions change from Case 2 to Case 3. The responses are shown in Fig. 12(a), 12(b), and 12(c), respectively.

The PID controller at winding section, which was tuned for a small roll, becomes detuned as the radius of the winding roll increases. The responses of t_3 and t_4 become sluggish as shown in Fig. 12(c).

The PID controller at the unwinding section, which was tuned for a large roll, becomes detuned as the radius of the unwinding roll decreases. The result of detuning is that the responses of t_1 and t_2 demonstrate a chattering instability after the start-up period is over as shown in Fig. 12(c). Such an instability may result in web breakage as the processing continues.

CONCLUSIONS

Start-up (or, shut-down) problems can be studied prior to system construction using first-principles modeling and digital simulation. It is essential that nonlinear models (rather than linearized models) be used in the analysis since start-up problems normally involve large variations of system roller velocities.

The two examples focused on studies of the PID control of tension in a web transport system during start up. Each PID controller was designed based on a (reduced) second-order linearized model and the pole assignment technique. For the system with load cells, second-order models were achieved by neglecting the dynamics of the load cell rollers. For the system with dancer subsystems, second-order models were achieved through the reduction of higher-order models.

For a load-cell-controlled system, web breakage could occur during start up if the system designed for one start-up condition is operated at a substantially different start-up condition as shown in Fig. 7(c). For a dancer-controlled system, system instability may occur after the start-up period is over as shown in Fig. 12 (c) and that may also result in web breakage.

The two examples demonstrate that fixed-gain PID control may be inadequate for operation over a broad range of start-up conditions. A more robust control technique would be to use variable-gain PID control.

REFERENCES

1. Hutton, M. F. and Rubins, M. J., "Simplification of High-Order Mechanical Systems Using the Routh Approximation", ASME Journal of Dynamic System, Measurement, and Control, 1975, pp. 383.
2. Kuo, B. J., Automatic Control Systems, Fourth Edition, Prentice Hall, Inc., 1982.
3. Reid, K. N., Shin, K. H., and Lin, K. C., "Variable-Gain Control of Longitudinal Tension in a Web Transport System", AMD-Vol. 149, Web Handling, ASME, 1992, pp. 87-100.
4. Reid, K. N. and Lin, K. C., "Dynamic Behavior of Dancer Subsystems in Web Transport Systems", to be presented in IWEB, 1993.

APPENDIX

System conditions and parameter values for simulation

$R_2 = 0.091$ m (0.3 ft)
$J_2 = 0.011$ N-m-sec^2 (0.0076 ft-lbf-sec^2)
$R_3 = 0.182$ m (0.6 ft)
$J_3 = 0.171$ N-m-sec^2 (0.122 ft-lbf-sec^2)
$R_4 = 0.091$ m (0.3 ft)
$J_4 = 0.011$ N-m-sec^2 (0.0076 ft-lbf-sec^2)
$K_1 = K_3 = K_5 = 135.6$ N-m/amp. (100 ft-lbf/amp.)
$L_1 = L_2 = L_3 = L_4 = 3.05$ m (10 ft)
$E_1 = E_2 = E_3 = E_4 = 2.4 * 10^9$ (350,000 psi)
$h_1 = h_2 = h_3 = h_4 = 127$ microns (5 mil)
$b_1 = b_2 = b_3 = b_4 = 30.5$ cm (12 in.)
$t_{1i} = t_{2i} = t_{3i} = t_{4i} = 5.4$ kgf (12 lbf)
$t_1^* = t_4^* = 5.4$ kgf (12 lbf)
$\tau_s = 5$ seconds

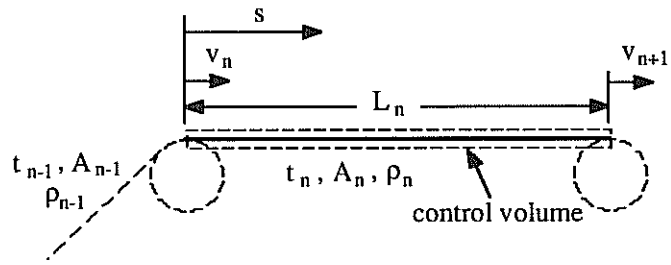

Fig. 1 Schematic of a Web Span

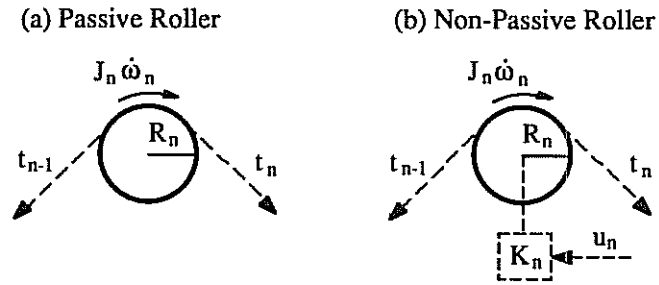

Fig. 2. Schematic of a Passive Roller and a Non-Passive Roller

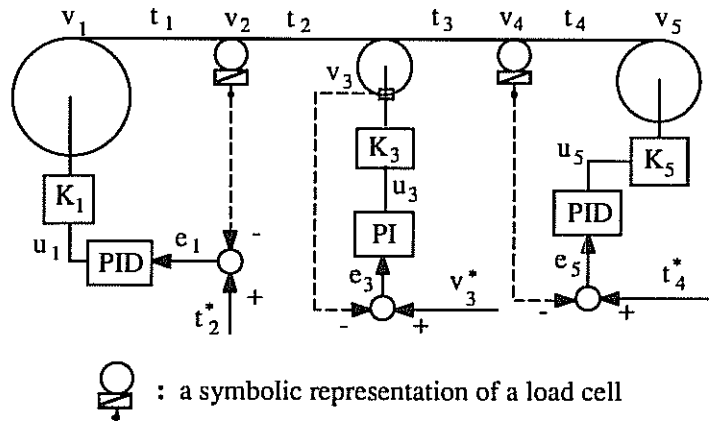

Fig. 3. A Web Transport System with Feedback Control of Web Tension and Load Cells for Tension Measurement

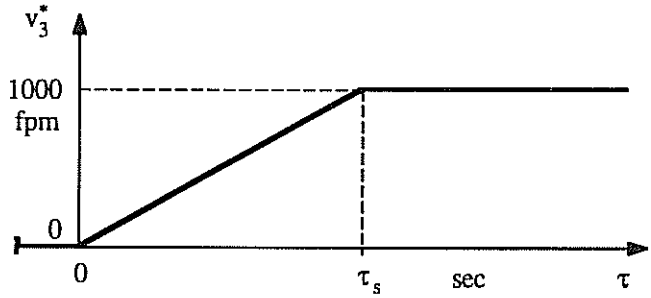

Fig. 4. Reference Velocity and Start-Up Time, τ_s

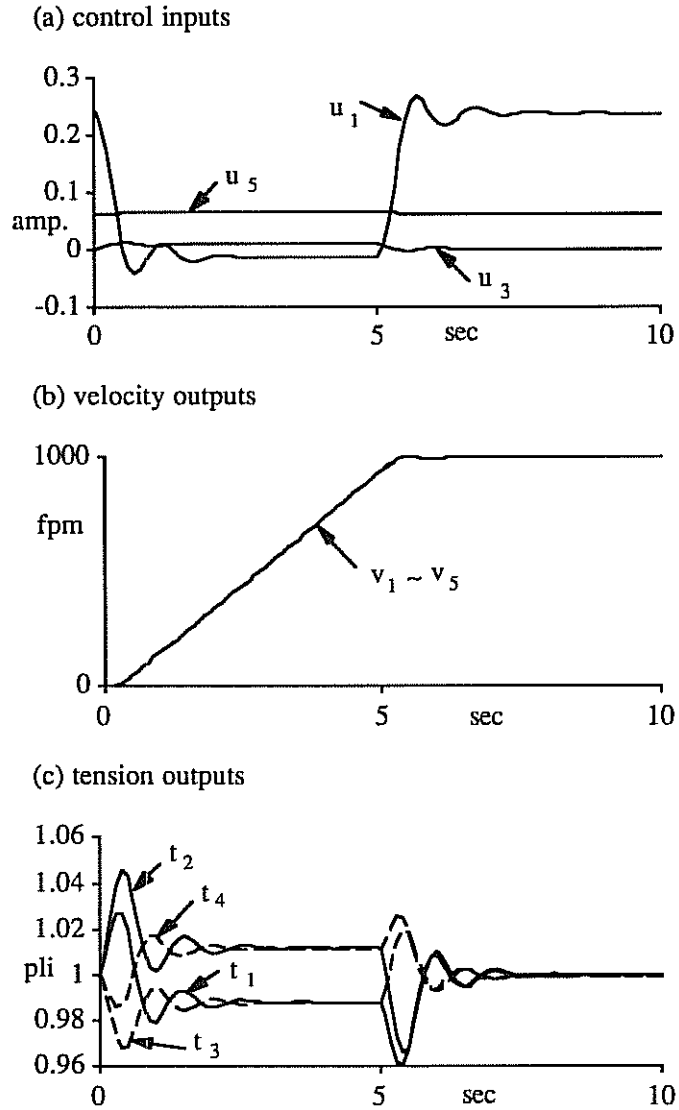

Fig. 5. Time Responses of System Inputs and Outputs, Example 1 - Case 1

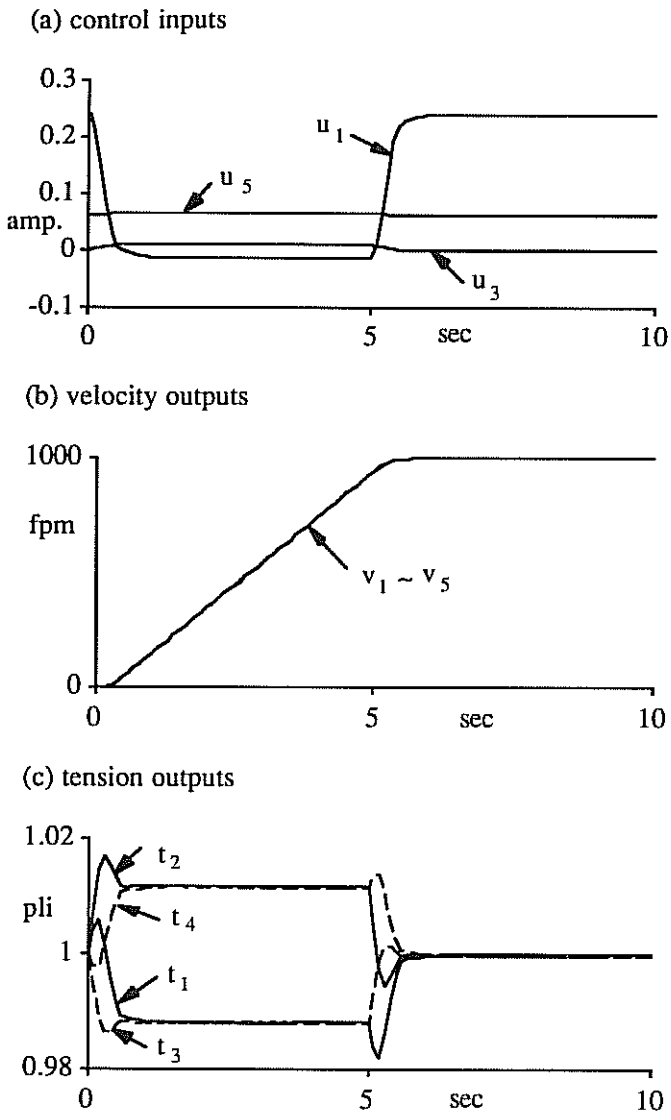

Fig. 6. Time Responses of System Inputs and Outputs, Example 1 - Case 2

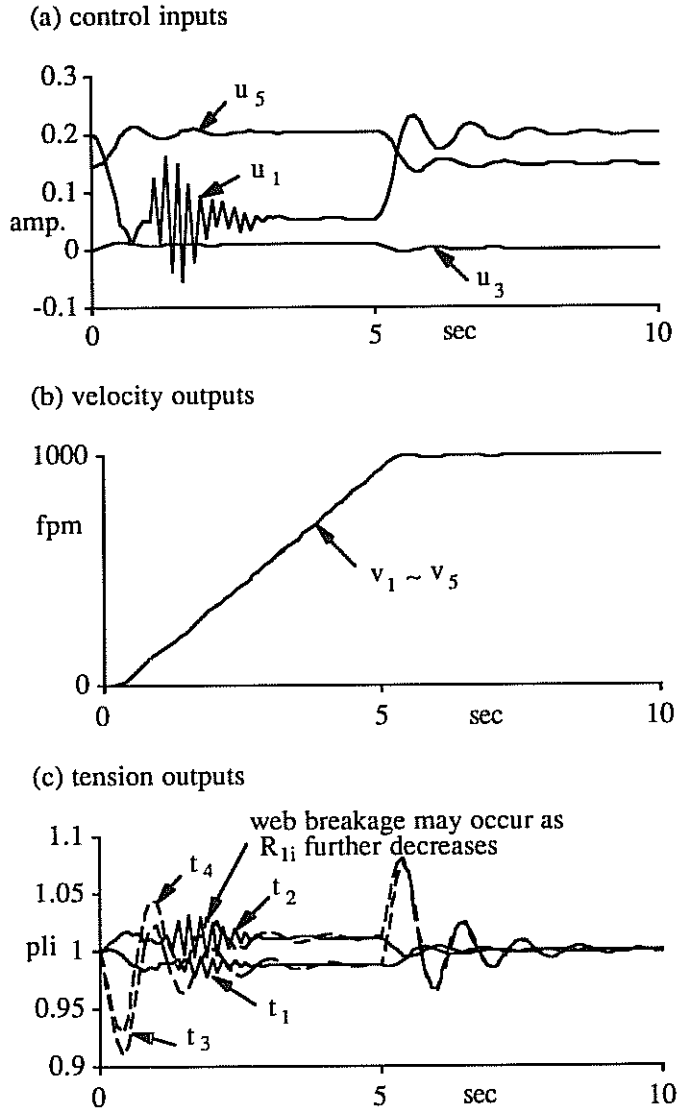

Fig. 7. Time Responses of System Inputs and Outputs, Example 1 - Case 3

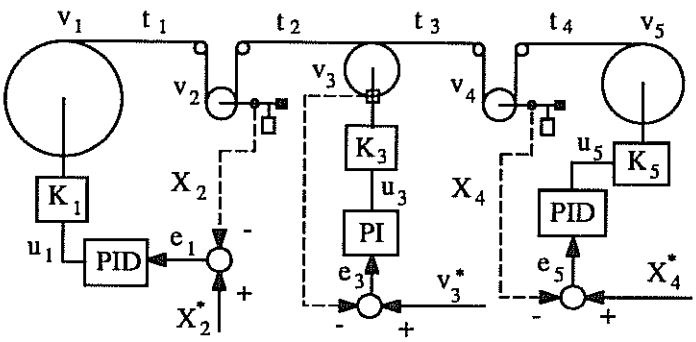

Fig. 8. A Web Transport System with Feedback Control of Web Tension and Dancer Subsystems for Tension Measurement

(a) a schematic diagram of a pivoting dancer subsystem

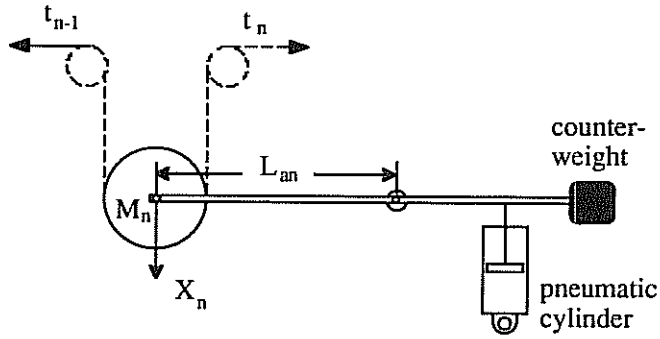

(b) a symbolic representation of a pivoting dancer subsystem

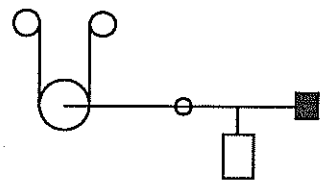

Fig. 9. Schematic and Symbolic of a Pivoting Dancer Subsystem

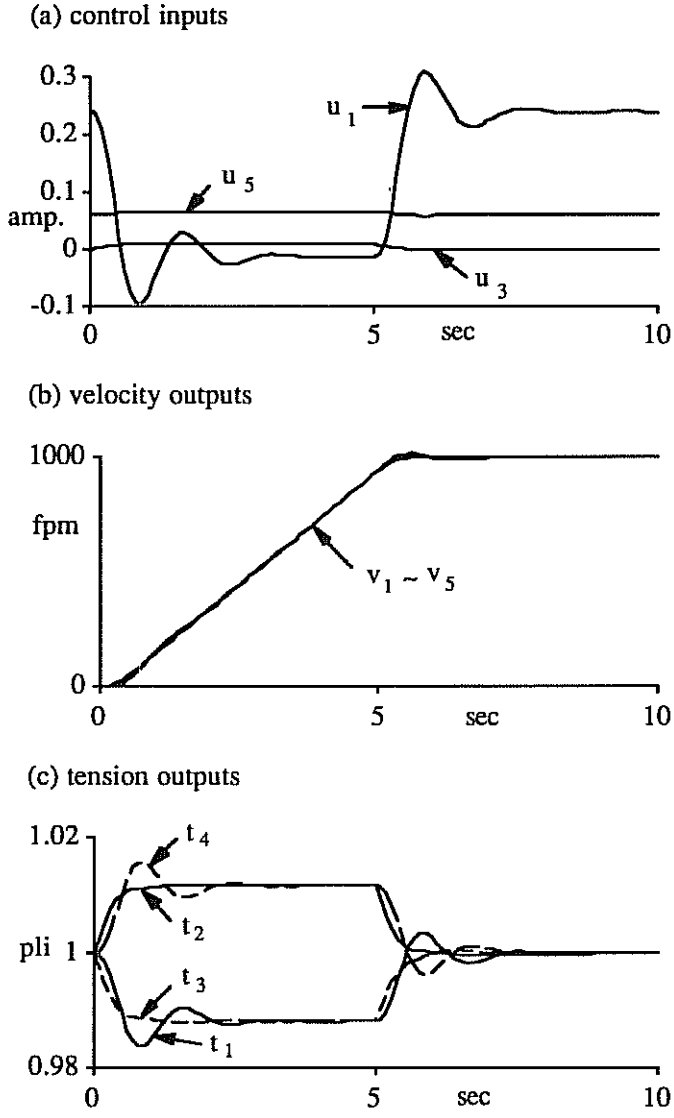

Fig. 10. Time Responses of System Inputs and Outputs, Example 2 - Case 1

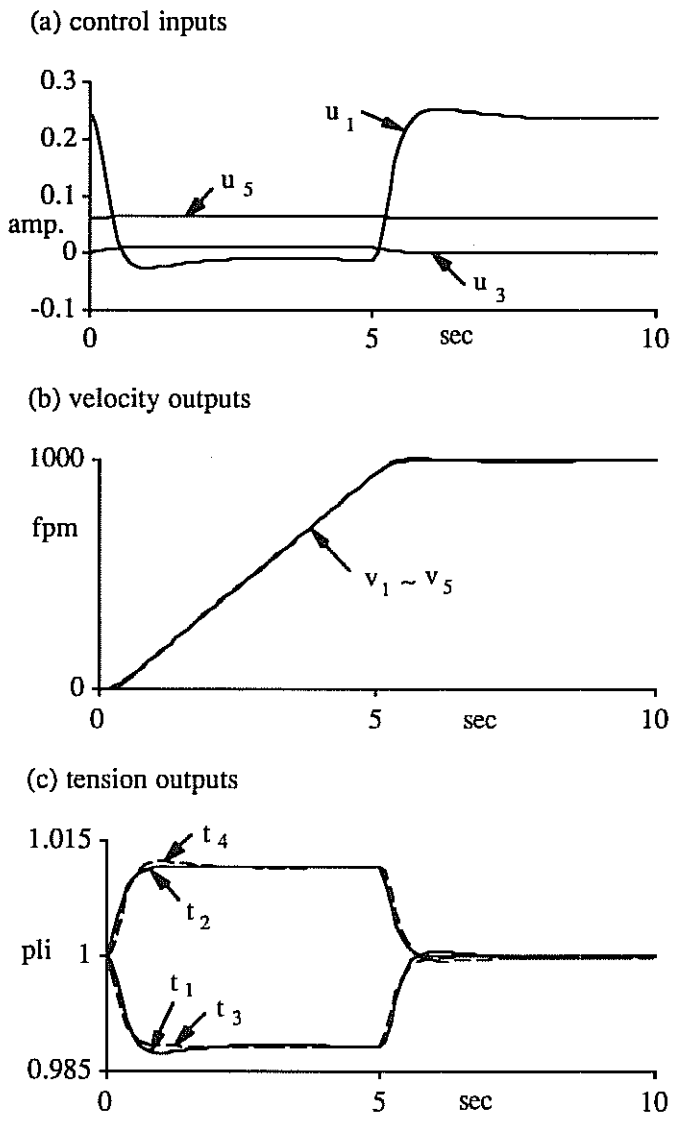

Fig. 11. Time Responses of System Inputs and Outputs, Example 2 - Case 2

(a) control inputs

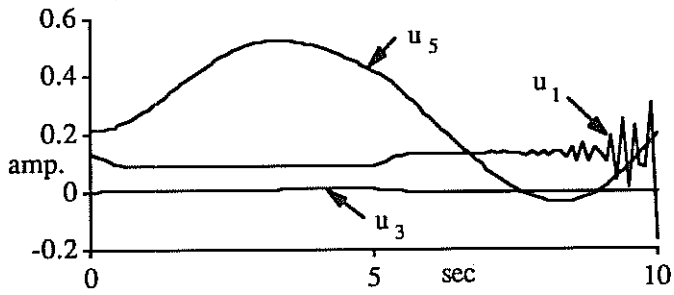

(b) velocity outputs

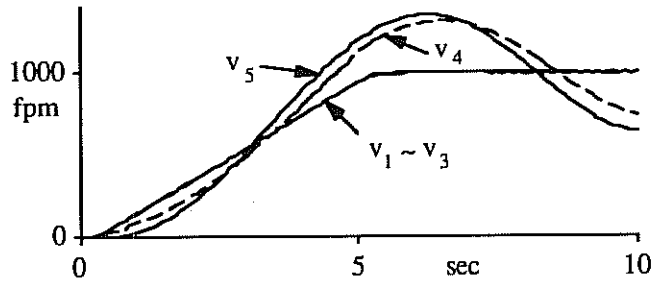

(c) tension outputs

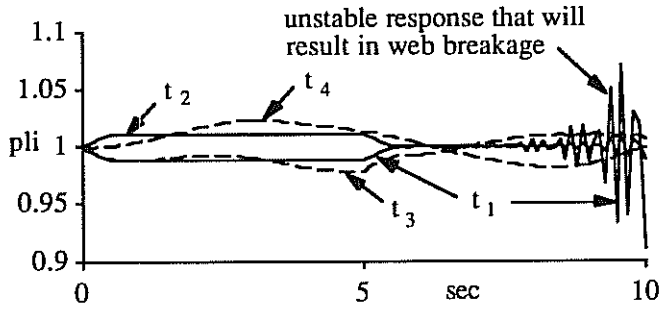

Fig. 12. Time Responses of System Inputs and Outputs, Example 2 - Case 3